Mott transition in three-orbital Hubbard model with orbital splitting

Tomoko Kita,[1,*] Takuma Ohashi,[2] and Norio Kawakami[1]
[1]*Department of Physics, Kyoto University, Kyoto 606-8502, Japan*
[2]*Department of Physics, Osaka University, Toyonaka, Osaka 560-0043, Japan*
(Received 19 May 2011; revised manuscript received 27 August 2011; published 28 November 2011)

We study the Mott transition in the three-orbital Hubbard model. To investigate how the orbital level splitting and the Ising-type Hund's coupling affect the Mott transition in the case of two electrons per site, we use the dynamical mean-field theory combined with continuous-time quantum Monte Carlo simulations. The calculation of the double occupancy reveals that the critical interaction strength separating a metallic phase and two kinds of insulating phases shows a nonmonotonic behavior as a function of the level splitting. We find that this behavior is characteristic for 1/3 filling, in comparison with the preceding results for different fillings and for two-orbital models. Strong competition between the two insulators results in an intriguing first-order transition to an insulating phase having intermediate characters between Mott and band insulators. It is also found that the two insulators show different behaviors in the phase boundary with the metallic phase in the interaction-temperature plane, which is reflected in a difference in the quasiparticle behavior around the transition. We also discuss the orbital selective Mott transition for larger Hund's coupling, which is compared with previous study at zero temperature.

DOI: 10.1103/PhysRevB.84.195130 PACS number(s): 71.30.+h, 71.10.Fd, 71.27.+a

I. INTRODUCTION

Strongly correlated electron systems with multiorbital degrees of freedom have been studied extensively. In these systems, orbital fluctuations enhanced by electron correlations induce a variety of intriguing phenomena, such as magnetic and/or orbital ordering, metal-insulator transition, etc. One of the hot topics is the newly discovered iron-based superconductors,[1] for which the orbital degrees of freedom play a key role in understanding the mechanism of superconductivity. It has also been elucidated that the Hund's coupling affects the system considerably, and orbital-dependent phenomena are essential in these systems.[2–5]

The orbital selective Mott transition (OSMT), where some of the orbitals become localized while the others still remain itinerant, is a typical phenomenon induced by the interplay of multiorbital effects and strong electron correlations.[6,7] The dynamical mean-field theory (DMFT) has been applied to the two-orbital Hubbard model with different bandwidths, and it has been clarified that the Hund's coupling plays an important role in the OSMT.[8–11] More recently, the OSMT has also been addressed in the system with the same bandwidths;[12,13] it has been suggested that the OSMT may occur in a three-orbital Hubbard model when the orbital degeneracy is lifted into doubly degenerate orbitals and a single orbital. In the doubly degenerate orbitals, a metallic state is expected to be further stabilized by orbital fluctuations than in a nondegenerate orbital. Therefore, separate transitions to the Mott insulating phase could occur in this system. However, it is not clear how the OSMT occurs in this system, and there are still few theoretical studies on the models with more than two orbitals.[12–17] As regards the Mott transition in the multiorbital systems,[18–21] it is known that the orbital degeneracy causes a sort of frustration and thus enhances orbital fluctuations, making the metallic state more stable against the Mott transition.[22,23] It is thus important to figure out how the orbital level splitting, which lifts the orbital degeneracy,[24,25] affects the Mott transition. Another important effect of the orbital level splitting is that it induces competition with the Hund's coupling[26] and thereby changes the nature of the Mott transition when the size of the splitting becomes comparable to the Hund's coupling. These facts naturally motivate us to study the Mott transition in the three-orbital Hubbard model by systematically changing the orbital level splitting and the Hund's coupling.

In this study, we investigate the Mott transition in the three-orbital Hubbard model with particular focus on how the Ising-type Hund's coupling and the orbital level splitting affect the Mott transition in the case of two electrons per site. For this purpose, we use DMFT combined with a continuous-time quantum Monte Carlo (CT-QMC) method as a solver of the effective impurity problem.[27–29] It is elucidated that the critical interaction strength for the metal-insulator transition shows a nonmonotonic behavior as the level splitting is changed. This is caused by two effects due to the level splitting: the reduction of orbital degeneracy and the competition with the Hund's coupling. We find that this behavior is characteristic for 1/3 filling, in comparison with the previous results obtained at different fillings[15] and for two-orbital models.[24–26] In some parameter regions, two kinds of insulating phases compete with each other, resulting in an unusual first-order transition to an insulating phase having intermediate characters between the Mott insulator (MI) and the band insulator (BI): within the insulating phase at finite temperatures, a crossover occurs in the physical quantities between the two insulating phases. By plotting critical interaction strength in the interaction-temperature plane, we find that the two insulators show different behaviors in the phase boundary with the metallic state. This difference is reflected in the density of states (DOS) for the metallic states around the transition. With increasing temperature, the quasiparticle state around the transition to the MI is suppressed, while the quasiparticle state near the correlated BI is rather enhanced. We also discuss the orbital selective Mott transition for larger Hund's coupling, comparing with the previous study at zero temperature.[12]

This paper is organized as follows. In the next section, we introduce the three-orbital Hubbard model and briefly mention

the method. In Sec. III, we explain the details of our results. A brief summary is given in Sec. IV.

II. MODEL AND METHOD

We consider the three-orbital Hubbard model defined by

$$H = -t \sum_{\langle i,j\rangle,\alpha,\sigma} c^{\dagger}_{i\alpha\sigma} c_{j\alpha\sigma} + \sum_{i,\alpha,\sigma} (-\mu + \Delta_{\alpha}) n_{i\alpha\sigma} + U \sum_{i,\alpha} n_{i\alpha\uparrow} n_{i\alpha\downarrow} + \sum_{i,\alpha\neq\alpha',\sigma,\sigma'} (U' - \delta_{\sigma\sigma'} J) n_{i\alpha\sigma} n_{i\alpha'\sigma'}, \quad (1)$$

where $c^{(\dagger)}_{i\alpha\sigma}$ is an annihilation (creation) operator of an electron with spin σ ($=\uparrow,\downarrow$) and orbital α ($=1,2,3$) at the ith site, and $n_{i\alpha\sigma} = c^{\dagger}_{i\alpha\sigma} c_{i\alpha\sigma}$ is the number operator. Here, t is the nearest-neighbor-hopping integral, μ is the chemical potential, and Δ_{α} is the energy level for orbital α. In the interaction terms, $U(U')$ is the intraorbital (interorbital) Coulomb interaction, and J is the Hund's coupling. We impose the condition $U = U' + 2J$ as usual. For simplicity, we use an Ising-type Hund's coupling, not including the spin-flip and pair-hopping terms. We fix the electron filling per site as $n = 2$ (referred to as 1/3 filling) to focus on the Mott transition in the case of two electrons per site. Orbital level splitting is given by Δ_{α} and we set $\Delta_1 = \Delta_2 = 0$, $\Delta_3 = -\Delta$ so that the energy level of doubly degenerate orbitals 1 and 2 is higher than that of the single orbital 3.

To investigate the Mott transition in this model, we use the single-site DMFT.[27] In the framework of DMFT, the lattice model is mapped onto an effective impurity model, where local electron correlations are taken into account precisely. The lattice Green's function is obtained via a self-consistency condition imposed on the impurity problem. In this paper, we use a semicircular DOS, $\rho(\omega) = (2/\pi D)\sqrt{1-(\omega/D)^2}$, which corresponds to the infinite-coordination Bethe lattice. We choose the energy unit as $D = 1$ (half bandwidth). To solve the effective impurity problem, we use the hybridization expansion CT-QMC method.[28,29] This method allows us to access the strong interaction regime in a wide range of temperatures, especially down to a very low temperature.[30–32] It is possible to determine the ground-state properties by extrapolating the temperature dependence of the data.[28,29] However, actual calculations have been done at finite but very low temperature successfully in a number of previous CT-QMC studies.[14–16,28,29] Therefore, we investigate the Mott transition in our three-orbital model and discuss the temperature dependence around the transition by using the DMFT combined with the CT-QMC. We iterate the DMFT self-consistent loop until the convergence is achieved within 40 times at most. In each iteration, we have typically performed 2×10^8 QMC samplings to reach sufficient computational accuracy at a very low temperature, $T/D = 0.02$.

Let us here briefly comment on the Hund's coupling in the Hamiltonian (1), without spin-flip and pair-hopping terms. Regarding the simultaneous Mott transition, which is mainly discussed in our paper, we expect that these terms do not qualitatively change the results for the following three reasons. First, the order of the Mott transition does not depend on whether the Hund's coupling is Ising-type or isotropic.[33] In previous studies of the two-orbital model with the same bandwidths at half filling, the effect of the Hund's coupling on the Mott transition at zero temperature has been investigated and it has been clarified that both types of Hund's coupling induce the first-order Mott transition.[11,21,36–38,46] Second, the effects of both types of Hund's coupling on the critical interaction of the Mott transition are qualitatively the same. In the two-orbital Hubbard model, both of them suppress it.[38] In addition, in the triply degenerate Hubbard model, the result for our model with the Ising-type Hund's coupling is consistent with that for the model with the isotropic Hund's coupling,[13,39] as mentioned below. Third, in the two-orbital Hubbard model, the effect of the competition between the orbital level-splitting and the isotropic Hund's coupling on the critical interaction[26] has been well reproduced by using the Ising-type Hund's coupling.[40] Therefore, we expect that, for our main purpose, to investigate the effects of the Hund's coupling and the orbital level-splitting on the simultaneous Mott transition at finite temperatures, spin-flip and pair-hopping terms are not important and do not qualitatively change our results.

However, these terms are known to be important around the OSMT at least in a two-orbital Hubbard model with different bandwidths; some studies have indicated that the Ising-type Hund's coupling suppresses the orbital selective Mott insulator (OSMI) phase,[41,42] and some other studies have investigated characteristic behavior of the OSMI phase in the system with the Ising-type Hund's coupling, non-Fermi-liquid behavior,[10,43,44] which has not been reported in the system with the isotropic Hund's coupling. In the three-orbital model with the same bandwidths we have used in this study, the effects of these terms on the OSMT have not been clarified so far. Therefore, in the next section, we will compare our results around the OSMT with that of the similar model with the isotropic Hund's coupling solved by the DMFT combined with exact diagonalization.[12] Still, in order to elucidate the effects of the difference between the Ising-type and isotropic Hund's couplings on the OSMT, further investigations are required, such as the introduction of the isotropic Hund's coupling to our framework, comparison of the Ising Hund's coupling with the isotropic one, etc.

III. RESULTS

A. Simultaneous Mott transition

Let us now investigate the Mott transition in the three-orbital Hubbard model at 1/3 filling (two electrons per site). In the main part of this section, we fix a strength of the Hund's coupling at $J/U = 0.05$. In Fig. 1(a), we show the double occupancy $D_{\rm occ} = \frac{1}{N_{\rm com}} \sum_{(\alpha,\sigma)\neq(\alpha',\sigma')} \langle n_{\alpha\sigma} n_{\alpha'\sigma'} \rangle$ computed for various Δ as a function of U at very low temperature $T/D = 0.02$. Here, $N_{\rm com}$ is the number of possible combinations of spin/orbital internal degrees of freedom. In our model, electrons have six internal degrees of freedom, two (three) for spin (orbital), therefore $N_{\rm com} = 15$. It is seen that the double occupancy monotonically decreases with increasing U. It shows coexistent solutions around the characteristic value of interaction U_c and is almost independent of U for larger interactions than U_c, indicating that the metal-insulator

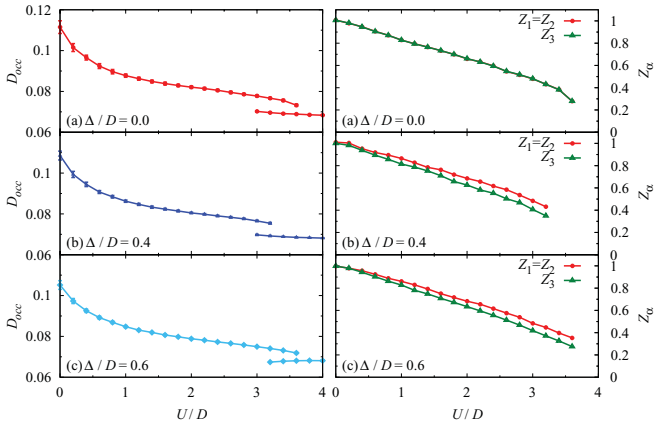

FIG. 1. (Color online) (a) Double occupancy $D_{\rm occ}$ and (b) renormalization factor in orbital α, Z_α, as a function of interaction strength U for several choices of level splitting Δ at temperature $T/D = 0.02$. Hund's coupling is fixed as $J/U = 0.05$. We find hysteresis in $D_{\rm occ}$, indicating the first-order Mott transition.

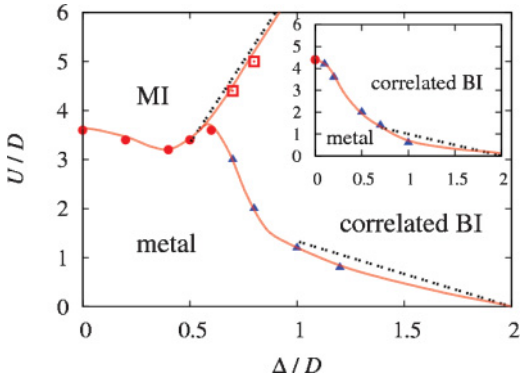

FIG. 2. (Color online) Δ-U phase diagram for the three-orbital Hubbard model at 1/3 filling ($n = 2$) with $J/U = 0.05$ and $T/D = 0.02$. The characteristic interaction strength U_{c_2} from the metal to the MI (correlated BI) insulating state is denoted by filled circles (triangles), and the crossover point from the correlated BI to the MI is denoted by open squares. Solid lines are to guide the eye. Dotted lines denote the phase boundaries obtained by simple estimations (see text). Inset shows the phase diagram for the model with $J = 0$.

transition occurs at U_c.[34] We find hysteresis for $\Delta/D = 0, 0.4$, and 0.6, which characterizes the first-order Mott transition.

To clarify the quasiparticle properties around the Mott transition, we also calculate the renormalization factor of orbital α, Z_α, which is defined as $Z_\alpha = [1 - \frac{\partial {\rm Im}\Sigma_\alpha(i\omega_n)}{\partial \omega_n}|_{\omega_n \to 0}]^{-1}$. We extrapolate Z_α from the imaginary frequency data of ${\rm Im}\Sigma_\alpha(i\omega_n)$ for small n with the use of third-order polynomials. In Fig. 1(b), the renormalization factors $Z_1(=Z_2)$ and Z_3 are shown as a function of U. To see the renormalization of the quasiparticle in the metallic phase, we show Z_α only for interaction strengths smaller than U_{c_2} defined by the metal-insulator transition with increasing U.[34] The renormalization factors monotonically decrease with increasing U. It is seen that the difference between $Z_1(=Z_2)$ and Z_3 is not relevant, resulting in a simultaneous Mott transition in this case.

By plotting the characteristic interaction strength U_{c_2} as a function of the level splitting Δ, we obtain the Δ-U phase diagram shown in Fig. 2. In the phase diagram, a nonmonotonic behavior appears in the Δ dependence of the critical interaction strength. We will clarify the origin and some implications of this characteristic behavior. For $\Delta = 0$, the ordinary Mott transition occurs, where two electrons are accommodated equally in the triply degenerate orbitals.[14,21] Finite Δ lifts triply degenerate orbitals, leading to the suppression of the metallic phase, which is accompanied by a slight decrease in the critical interaction strength, as seen for $\Delta/D < 0.4$. In such a small Δ region, the Hund's coupling dominates the effect of Δ, resulting in a MI with the electron number in each orbital $(n_1 + n_2, n_3) = (1,1)$, where n_α denotes the electron number in orbital α, to gain the energy due to the Hund's coupling with a parallel spin alignment. On the other hand, for a large Δ region, another insulating phase is stabilized, which is adiabatically connected to a BI specified by $(n_1 + n_2, n_3) = (0,2)$. This insulating phase is referred to as a correlated BI in this study. However, in the limit of large U, the MI is realized in the entire Δ region, because J is large there (recall the condition of $J/U = 0.05$). Filled triangles (open squares) in Fig. 2 denote the critical interaction strength of the phase transition (crossover) from the metal to the correlated BI (from the correlated BI to the MI). We find that, for $\Delta/D > 0.4$, the interaction strength of transition to the MI (filled circles and open squares) is enhanced with Δ as a result of the competition between the Hund's coupling and the orbital level splitting. In the atomic limit of the effective impurity problem within DMFT, the energies of J-induced high spin states with fourfold degeneracy and a Δ-induced singlet are degenerate when $3J = \Delta$. We draw the line of $3J = \Delta$ in the phase diagram as a guide to the transition line between the correlated BI and the MI. At lower temperatures, the crossover observed at $T/D = 0.02$ is expected to change into a first-order transition. For large Δ ($\Delta/D > 0.7$), the critical interaction strength of phase transition to the correlated BI decreases with increasing Δ. In the limit of $\Delta \to 2D$ (bandwidth), the phase boundary is simply estimated by the mean-field theory at zero temperature as $U = (2 - \Delta)/0.75$, which is qualitatively in good agreement with our results.

Summarizing, the level splitting Δ has two important effects: (i) Δ lifts the degeneracy of triply degenerate orbitals and (ii) it induces the competition with J. When these effects are equally relevant, the first-order transition occurs between the two insulating phases. Around this transition, orbital fluctuations are effectively enhanced, and therefore the metallic state is stabilized, giving rise to the nonmonotonic Δ dependence of the critical interaction strength for the Mott transition.

For comparison, we show the Δ-U phase diagram for $J = 0$ in the inset of Fig. 2. In this case, the splitting Δ simply lifts the degeneracy of triply degenerate orbitals, leading to the monotonic decrease of the critical interaction strength as a function of Δ. Note that the correlated BI is realized in the entire Δ regime except for $\Delta = 0$, where the transition point $U_{c_2}/D \sim 4.4$ is much larger than that for finite J ($U_{c_2}/D \sim 3.6$ for $J/U = 0.05$) because of the high degeneracy due to spin-orbital symmetry at $U = U'$.

Before closing this subsection, we briefly comment on the filling dependence of the nonmonotonic behavior of U_c as a function of Δ, which is induced by the two effects of Δ as mentioned above. We have found that this behavior is characteristic for 1/3 filling, in comparison with previous results for different fillings and for two-orbital models. For the three-orbital system with one electron per site ($n = 1$),[15] the nonmonotonic behavior of U_c does not appear because the Hund's coupling is not important for $n = 1$ and the competition between J and Δ does not occur. Therefore, the effect of Δ is only the former one; Δ just lifts the orbital degeneracy and U_c monotonically decreases with increasing Δ. This behavior is qualitatively similar to that in the two-orbital model at quarter filling, namely $n = 1$.[24,25] For $n = 3$,[15] at half filling, the competition between Hund's coupling and orbital level splitting occurs but the phase diagram in the small Δ region shows a different behavior from that for $n = 2$. At half filling, the former effect of Δ, lifting the orbital degeneracy, is completely obscured by the Hund's coupling acting on three electrons which occupy three orbitals. As a result, the effect of Δ is only the latter one; Δ competes with J, which results in the increase of U_c with increasing Δ, as shown in the half-filled case in the two-orbital model.[26] For $n = 4$, the competition between Δ and J does not occur. For finite Δ, the system is effectively reduced to a doubly degenerate two-orbital model because the lowest orbital is almost fully occupied by two electrons. Consequently, U_c monotonically decreases with increasing Δ. For the model with $n = 5$, the competition between Δ and J does not occur for the same reason as in the case of $n = 1$, and U_c monotonically decreases with increasing Δ. Therefore, in our model, the nonmonotonic behavior of U_c as a function of Δ only appears at filling $n = 2$.

B. Temperature dependence

The two insulating states in Fig. 2, the MI and the correlated BI, show different behaviors at finite temperatures. In Fig. 3, we show the U-T phase diagram for several choices of Δ. In Fig. 3(a), for $\Delta = 0$, we can see a first-order transition (filled circles) between the metal and the MI at low temperatures, while it becomes a crossover (open circles) at higher temperatures. Note that the coexistence region exists between U_{c1} and U_{c2} at low temperatures.[34] It is seen that the metal rather than the MI is stabilized at low temperatures, which is due to higher entropy of the MI with localized spin and orbital degrees of freedom. This phase diagram is similar to that for the single-band Hubbard model treated by the DMFT,[27] for which the insulating phase is stabilized at lower temperatures.

On the other hand, two separate phase transitions occur for large level splitting, $\Delta/D = 0.8$, as shown in Fig. 3(c); with increasing U, the transition occurs first from the metal to the correlated BI and then from the correlated BI to the MI. We note that the former transition shows a different behavior from that for $\Delta = 0$ in Fig. 3(a); the correlated BI is stabilized at lower temperatures. This is because the correlated BI, which is adiabatically connected to a BI, has small entropy compared with the metallic state.

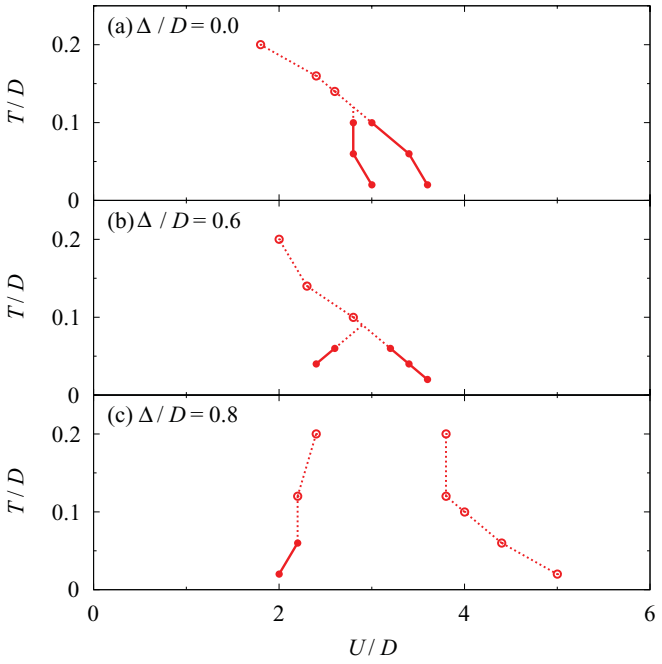

FIG. 3. (Color online) U-T phase diagram for the three-orbital Hubbard model at 1/3 filling with $J/U = 0.05$ for several choices of Δ. Filled (open) circles denote the first-order transitions (crossovers). Lines are to guide the eye.

For the intermediate level splitting, as seen in Fig. 3(b) for $\Delta/D = 0.6$, a single metal-insulator transition with both characteristics mentioned above appears; the transition at U_{c_2} with increasing U is from the metal to the MI, which is similar to that in the single-band Hubbard model. On the other hand, the phase transition at U_{c_1} with decreasing U shows a similar behavior to that of the correlated BI-to-metal transition; the insulating phase is located in the temperature regime lower than the metallic phase. This is because the crossover occurs in the insulating phase from the MI to the correlated BI as U decreases (i.e., J decreases). For slightly larger U than U_{c_1}, the system is in the correlated BI with small entropy, making the slope featured by U_{c_1} quite different from that of U_{c_2}. Detailed discussions on the physical quantities in this intermediate case will be given in the next subsection.

Numerically, in the correlated BI in Fig. 3(c), it is hard to perform the DMFT calculation within the same accuracy as in the other phases, because the upper orbitals are almost empty, $n_1(n_2) \sim 0$, which reduces the accuracy of the Green's functions and the hybridization functions. Therefore, it is not easy to figure out whether the hysteresis exists or not on both sides of the correlated BI in Fig. 3(c), although we find that the transitions at lower temperature are of first order.

To see how the quasiparticles around the transitions to each insulator evolve with changing the temperature, we also calculate the DOS in orbital α, $\rho_\alpha(\omega)$ by applying the maximum entropy method (MEM)[45] to the imaginary-time QMC data. In Figs. 4(a) and 4(b), we show the orbital-dependent DOS for $\Delta/D = 0.4$, $U/D = 3.2$ ($\Delta/D = 0.8$, $U/D = 2.0$), the metallic state around the transition to the MI (correlated BI). Each DOS is shown for different temperatures, at very low temperature, $T/D = 0.02$, the same as the

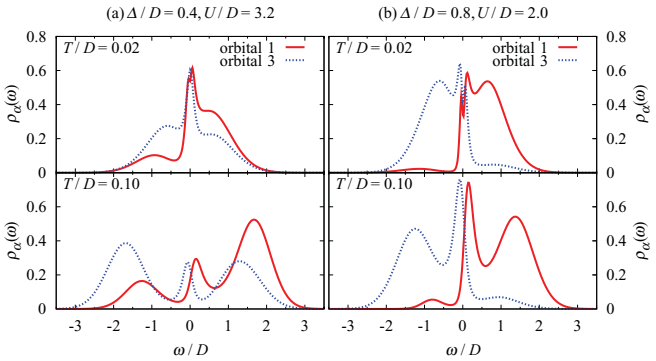

FIG. 4. (Color online) Density of states for (a) $\Delta/D = 0.4$, $U/D = 3.2$ and (b) $\Delta/D = 0.8$, $U/D = 2.0$ at different temperatures $T/D = 0.02, 0.10$ with $J/U = 0.05$.

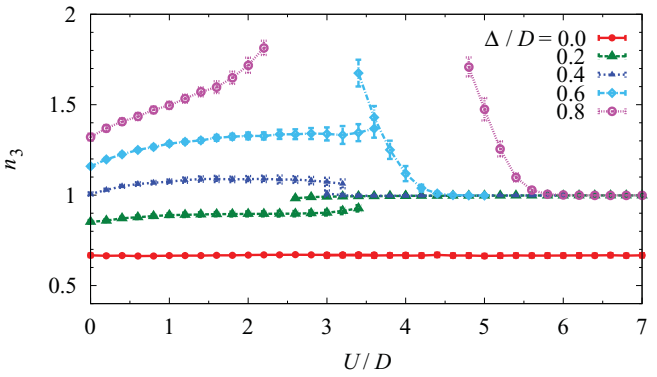

FIG. 5. (Color online) Electron number in the lower orbital 3, n_3, as a function of U for several choices of Δ with $J/U = 0.05$ and $T/D = 0.02$. Note that $n_1 + n_2 = 2 - n_3$.

temperature for the Δ-U phase diagram (Fig. 2), and rather higher temperature, $T/D = 0.10$. For the metallic state around the MI [Fig. 4(a)], it is seen that, at low temperature, the DOS for both orbitals form heavy quasiparticle peaks around the Fermi level, indicating the strongly renormalized state around the Mott transition. With increasing temperature, these quasiparticle peaks are suppressed. This behavior is consistent with the phase boundary between the metal and the MI in the U-T phase diagram [Fig. 3(a)]. On the other hand, for the metallic state around the transition to the correlated BI [Fig. 4(b)], it is seen that, at low temperature, sharp peaks are formed near the Fermi level, but they seem to exhibit gaplike behavior, which is expected to be a precursor to the transition to the correlated BI. With increasing temperature, these peaks are rather enhanced, differently from the behavior around the MI. Note that the low-energy quasiparticle peak is correctly computed by MEM while the distance of the two Hubbard peaks at $T/D = 0.02$ is much less than U/D, which might be an artifact due to MEM. We have confirmed that the DOS at the Fermi level obtained by MEM is consistent with that by the extrapolation of the Matsubara Green's function, $\rho_\alpha(\omega = 0) \sim -\lim_{\omega_n \to 0} \mathrm{Im}G(i\omega_n)/\pi$. Therefore, we believe that our discussions about the low-energy behavior of DOS are not influenced by an artifact due to MEM.

C. Effects of Hund's coupling

To see the nature of the Mott transition for each Δ more clearly, we calculate the electron number in each orbital α, $n_\alpha = \sum_\sigma \langle n_{\alpha\sigma} \rangle$. In Fig. 5, we show the electron number in the lower orbital 3, $n_3 = \sum_\sigma \langle n_{3\sigma} \rangle$, as a function of U. Since the total filling is fixed as $n = 2$, the electron number in degenerate orbitals 1 and 2 satisfies $n_1 + n_2 = 2 - n_3$. For $\Delta = 0$, n_3 is constant ($n_3 = 2/3$) because of triply degenerate orbitals. The level splitting Δ increases n_3 (decreases $n_1 + n_2$) at $U = 0$. For small Δ, e.g., $\Delta/D = 0.2$ and 0.4, n_3 slightly increases with U in the small U region. Around U_c, n_3 shows a discontinuity, and takes the value $n_3 = 1$ beyond U_c, implying that the system enters the MI. In Fig. 6, we show the spin-correlation function $\langle S_z^{(\mathrm{U})} S_z^{(\mathrm{L})} \rangle$ between the upper two orbitals and the lower orbital as a function of U. Here, $S_z^{(\mathrm{U})} = \sum_{\alpha=1,2} (n_{\alpha\uparrow} - n_{\alpha\downarrow})$ and $S_z^{(\mathrm{L})} = n_{3\uparrow} - n_{3\downarrow}$. It is seen that the spin correlation increases with U and is enhanced near the Mott transition. In the triply degenerate case ($\Delta = 0$), the value of $\langle S_z^{(\mathrm{U})} S_z^{(\mathrm{L})} \rangle$ jumps to 2/3 at the transition point because of $n_1 = n_2 = n_3 = 2/3$. As small orbital splitting ($\Delta/D = 0.2$ and 0.4) is introduced, $\langle S_z^{(\mathrm{U})} S_z^{(\mathrm{L})} \rangle$ jumps to 1 at the transition point, indicating that the ferromagnetic spin correlation due to the Hund's coupling is maximally enhanced in the MI. We find that the effect of the Hund's coupling is dominant in the vicinity of the Mott transition, which causes the enhancement of the spin correlation even in the metallic state.

For $\Delta/D = 0.8$, transitions occur twice; with increasing U, the transitions from the metal to the correlated BI and from the correlated BI to the MI occur. Note that we do not show data in the correlated BI phase because of the difficulty in numerical computations, as mentioned in the last subsection. In the metallic phase around the former transition, n_3 tends to approach 2, indicating that the system goes to the fully orbital-polarized state. In this case, the spin-correlation function [Fig. 6(e)] is not enhanced at all, which is different from that in the transition to the MI. By further increasing U, the crossover behavior between the correlated BI and the MI appears in these quantities; n_3 gradually decreases and approaches 1, and $\langle S_z^{(\mathrm{U})} S_z^{(\mathrm{L})} \rangle$ is enhanced to 1 [Fig. 6(f)].

For $\Delta/D = 0.6$, where both J and Δ are relevant and competitive with each other around the Mott transition, we find a remarkable effect due to the competition. In Fig. 5, for $\Delta/D = 0.6$, it is seen that n_3 increases with U, exhibits a discontinuity, and then takes a noninteger value, which changes continuously even in the insulating phase. Actually, the competition between J and Δ realizes a nontrivial insulating state with $(n_1 + n_2, n_3) \neq (1,1)$ and $(n_1 + n_2, n_3) \neq (0,2)$, which is also reflected in the spin-correlation function. In Fig. 6, we can see that $\langle S_z^{(\mathrm{U})} S_z^{(\mathrm{L})} \rangle$ increases with U, jumps to a value smaller than 1 at the transition, and then gradually approaches 1 with further increasing U. These characteristic properties in the insulating phase stem from a crossover between two distinct insulating states at finite temperatures [see Fig. 3(b)]: at the phase transition from the metallic side, the above physical quantities exhibit discontinuous changes to the intermediate values between those expected for the two insulating phases, which can then change continuously according to the values of U, J, Δ, etc.

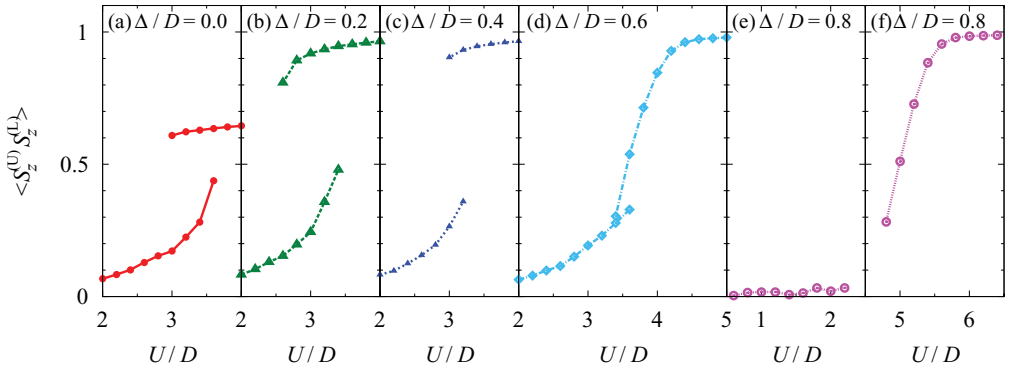

FIG. 6. (Color online) Interorbital correlation functions of spin $\langle S_z^{(U)} S_z^{(L)} \rangle$ as a function of U for several choices of Δ with $J/U = 0.05$ and $T/D = 0.02$.

D. Orbital selective Mott transitions

Finally, we investigate the Mott transition in the case of larger Hund's coupling. Remarkably, we find that the introduction of large Hund's coupling reveals an intriguing feature in the Mott transition, i.e., OSMT.[12] In Fig. 7, we show the Δ-U phase diagram for $J/U = 0.15$. It is seen that the large values of J stabilize the MI region, and the orbital selective Mott insulator (OSMI) phase emerges in it. In the phase diagram, the critical interaction of the first-order transition (crossover) is denoted by filled (open) circles, which is determined from the position of the jump or crossover in the double occupancy with increasing U. Note that the crossover behavior is due to the finite-temperature effects and all the phase boundaries shown in the figure should be of first order at zero temperature.

Let us start with the simple case of $\Delta = 0$ (the triply degenerate case) and discuss the J dependence of U_c. We first compare the three distinct values for the transition point at $\Delta = 0$, shown in Figs. 2 and 7, where the system undergoes a simultaneous Mott transition. By comparing the results in Fig. 2 (finite J) and the inset of Fig. 2 ($J = 0$) at $\Delta = 0$, it is seen that the introduction of J suppresses U_{c_2}. This is because J lifts the high degeneracy due to spin-orbital symmetry ($U = U'$), driving the system to the MI in Fig. 2, where a high-spin state with a parallel spin alignment is realized due to the Hund's coupling, as shown in the spin-correlation function (Fig. 6). However, further increase in J ($J/U = 0.15$ in Fig. 7) makes U_{c_2} larger again. This may be caused by the reduction of the Hubbard gap, which is roughly proportional to $U' - J$. This kind of nonmonotonic behavior in U_c is qualitatively consistent with results for the similar model with the isotropic Hund's coupling, including spin-flip and pair-hopping terms.[13,39] The transition temperature seems to be suppressed by the effect of J, and actually the crossover behavior emerges for $J/U = 0.15$ at $T/D = 0.02$ in Fig. 7.

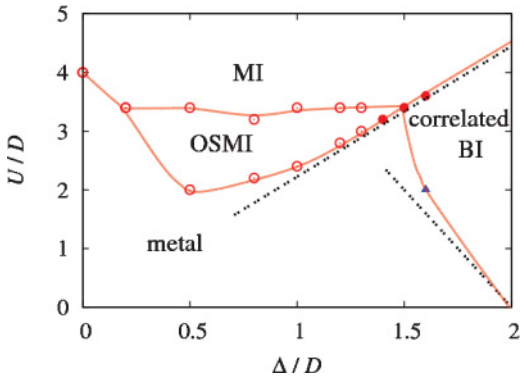

FIG. 7. (Color online) Δ-U phase diagram for the three-orbital Hubbard model at 1/3 filling with $J/U = 0.15$ and $T/D = 0.02$. The characteristic interaction strength from the metal to the MI (correlated BI) is denoted by circles (triangles). The critical interaction of the first-order transition (crossover) is denoted by filled (open) circles. We only show U_{c_2} for the first-order transition. Solid lines are to guide the eye. Dotted lines denote the phase boundaries obtained as a guide by similar estimations to the case for $J/U = 0.05$ (Fig. 2).

For finite Δ ($0.2 < \Delta/D < 1.5$), we find that the transition (or crossover) occurs twice at $U = U_c^{(L)}$ and $U = U_c^{(U)}$; i.e., the OSMT emerges. $U_c^{(U)}$ ($U_c^{(L)}$) is the characteristic interaction for the first (second) Mott transition.[34] Note that the Mott transition in the lower orbital occurs first at the smaller interaction, $U_c^{(L)} < U_c^{(U)}$, where the upper orbital is still metallic. As seen in the phase diagram in Fig. 7, $U_c^{(L)}$ is in good agreement with the line $J = 3\Delta$ drawn as a guide to the transition between the MI and the correlated BI, indicating that $U_c^{(L)}$ is indeed caused by the competition between J and Δ, similar to the case for $J/U = 0.05$. On the other hand, the characteristic interaction $U_c^{(U)}$ for the second Mott transition (upper orbitals) is almost independent of Δ. Actually, in the limit of large Δ, the second transition can be described effectively in terms of the two-orbital Hubbard model at quarter filling, where the Mott transition may be triggered by the reduced interaction $\sim U' - J$.[35] However, we find that the characteristic interaction $U_c^{(U)}/D \sim 3.4$ is much smaller than that expected for the two-orbital model at quarter filling for the same parameters ($J/U = 0.15$, $T/D = 0.02$), $U_{c_2}^{(2\mathrm{orb})}/D \sim 4.6$. This discrepancy is attributed to the Hund's coupling between electrons in the upper orbitals and the lower orbital, which substantially suppresses spin fluctuations in the upper orbitals and consequently reduces the value of $U_c^{(U)}$. For larger Δ ($\Delta/D \gtrsim 1.4$), the two separate transitions merge together again, leading to the simultaneous first-order transition.

To see how the quasiparticles evolve around the OSMT, we show the orbital-dependent DOS in Fig. 8 for $J/U = 0.15$, $\Delta/D = 0.8$. We show the DOS for three phases: the metal,

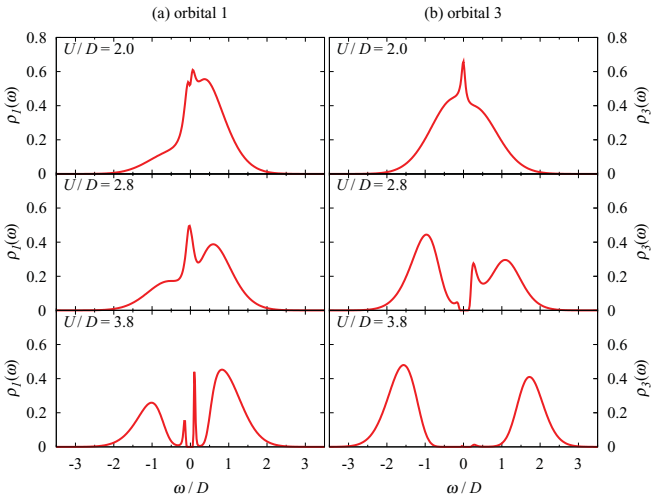

FIG. 8. (Color online) Density of states in (a) orbital 1 and (b) orbital 3 for several choices of U at $T/D = 0.02$ with $\Delta/D = 0.8$ and $J/U = 0.15$.

the OSMI, and the MI. In the metallic phase ($U/D = 2.0$), the quasiparticle peaks appear around the Fermi level in both orbitals. With increasing U, the system enters the OSMI phase ($U/D = 2.8$), where the DOS for the lower orbital 3 opens a gap while the DOS for the upper orbitals 1 and 2 are still metallic with the quasiparticle peak. In the MI phase ($U/D = 3.8$), the DOS for both orbitals open gaps. In Fig. 9, we show the imaginary part of the self-energy in the metallic and OSMI phases. In the metallic phase, the $\lim_{\omega_n \to 0} \mathrm{Im}\Sigma(i\omega_n)$ goes to 0 and shows Fermi-liquid behavior. On the other hand, in the insulating phase, $\mathrm{Im}\Sigma(i0)$ diverges. In the OSMT phase, $\mathrm{Im}\Sigma(i0)$ for orbital 1 tends to remain finite, indicating the non-Fermi-liquid behavior. This tendency is consistent with the previous study.[12]

In Fig. 10(a), we show the electron number of orbital 3, n_3, as a function of U for several choices of Δ. For finite Δ, we can see that n_3 dramatically increases or decreases toward a value of commensurate condition, $n_3 = 1$, and eventually has the fixed value $n_3 = 1$ beyond $U_c^{(\mathrm{L})}$. We observe a discontinuity in n_3 at the first-order transition for $\Delta/D = 1.5$ (though very small) and a continuous change characteristic of the crossover for $\Delta/D = 0, 0.2, 0.8$, and 1.2. In order to clarify how strongly the renormalization of the system parameters occurs around

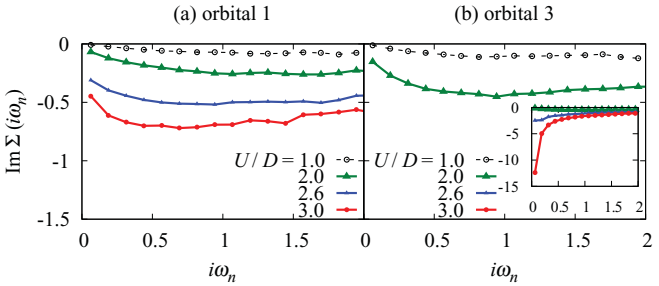

FIG. 9. (Color online) Imaginary part of self-energy in (a) orbital 1 and (b) orbital 3 for several choices of U at $T/D = 0.02$ with $\Delta/D = 0.8$ and $J/U = 0.15$.

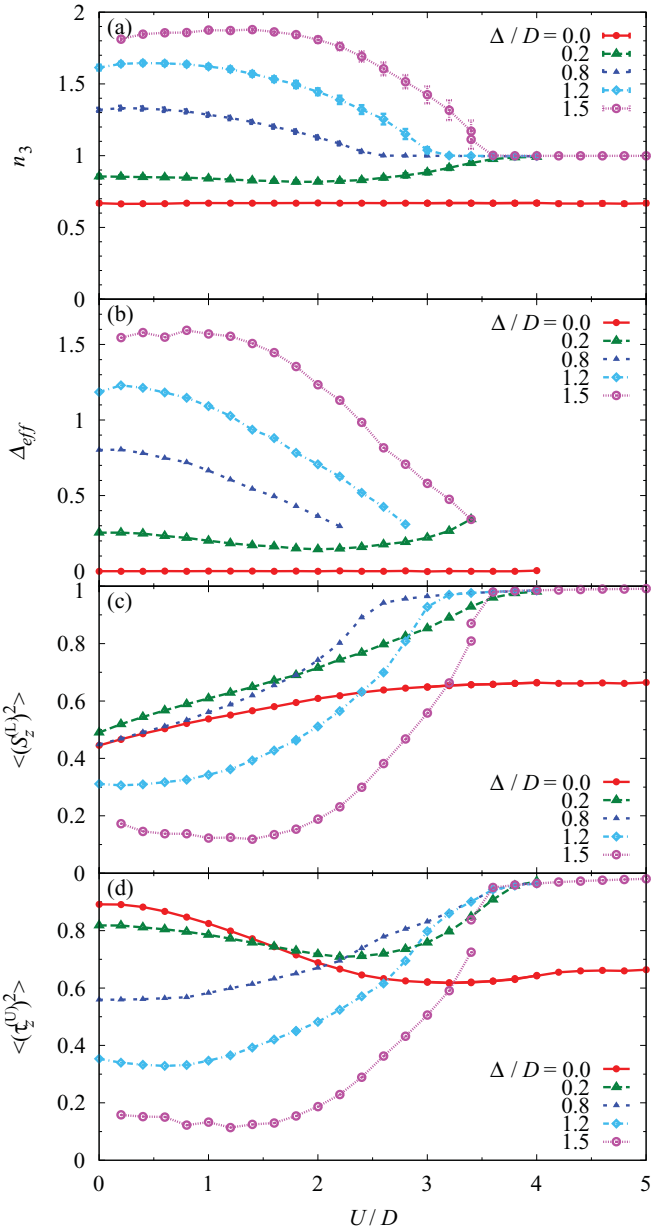

FIG. 10. (Color online) (a) Electron number in the lower orbital 3, n_3, (b) effective level splitting Δ_{eff}, (c) squared onsite spin moment in the lower band $\langle (S_z^{(\mathrm{L})})^2 \rangle$, and (d) squared onsite orbital moment in the upper bands $\langle (\tau_z^{(\mathrm{U})})^2 \rangle$ as a function of interaction strength U for several choices of level splitting Δ. Other parameters are set as $J/U = 0.15$ and $T/D = 0.02$.

the transition point, we calculate the effective level splitting Δ_{eff}, defined as

$$\Delta_{\mathrm{eff}} = \mu_3 - \mu_1, \tag{2}$$

$$\mu_1 = Z_1[\mu - \mathrm{Re}\Sigma_1(\omega = 0)], \tag{3}$$

$$\mu_3 = Z_3[\mu + \Delta - \mathrm{Re}\Sigma_3(\omega = 0)], \tag{4}$$

where μ_α is the effective chemical potential for the quasiparticles of orbital α, which incorporates the self-energy shift due to the interactions. We obtain $\mathrm{Re}\Sigma_\alpha(\omega = 0)$ from the imaginary frequency data $\mathrm{Re}\Sigma_\alpha(i\omega_n)$ for small n with a quadratic-function extrapolation scheme. In Fig. 10(b), we

show the U dependence of the computed $\Delta_{\rm eff}$. Note that we show $\Delta_{\rm eff}$ only for interaction strengths smaller than $U_c^{\rm (L)}$, since we are interested in the renormalization effects in the metallic phase. It is seen that $\Delta_{\rm eff}$ increases or decreases around $U_c^{\rm (L)}$, giving rise to the increase or decrease in the electron number n_3. From these results, we can say that the transition at $U = U_c^{\rm (L)}$ is mainly driven by the strong renormalization of the level splitting, resulting in a kind of *filling-control* Mott transition. On the other hand, the phase transition between the OSMI phase and the MI phase is driven by an *interaction-control* mechanism, and can be described effectively by a two-orbital Mott transition at quarter filling. As a result, the transition point is almost independent of Δ, though the value of the critical interaction is reduced by the Hund's coupling between different orbitals.

To characterize the OSMT, we further calculate the local moment of the spin and orbital. In Figs. 10(c) and 10(d), we show the squared spin-moment in the lower orbital $\langle (S_z^{\rm (L)})^2 \rangle$ and that of the orbital moment in the upper orbitals $\langle (\tau_z^{\rm (U)})^2 \rangle$, respectively. Here, $S_z^{\rm (L)} = n_{3\uparrow} - n_{3\downarrow}$, $\tau_z^{\rm (U)} = \sum_\sigma (n_{1\sigma} - n_{2\sigma})$. $S_z^{\rm (L)}$ ($\tau_z^{\rm (U)}$) is expected to take values close to 1 when the lower orbital (upper orbitals) becomes the Mott insulator with $n_3 = 1$ ($n_1 + n_2 = 1$). It is shown that $\langle (S_z^{\rm (L)})^2 \rangle$ is enhanced around the first transition at $U = U_c^{\rm (L)}$ and indeed takes a value close to 1 beyond $U_c^{\rm (L)}$, which is consistent with the behavior in the electron number n_3 and the effective level splitting $\Delta_{\rm eff}$. On the other hand, for $\Delta/D = 0.8$ and 1.2, where OSMT occurs, the value of $\langle (\tau_z^{\rm (U)})^2 \rangle$ is still less than 1 even at $U = U_c^{\rm (L)}$, but increases with further increasing U, and finally takes the value close to 1 beyond $U_c^{\rm (U)}$ (the second transition point). This implies that, in the OSMI phase, the orbital fluctuations play an important role in stabilizing the coexistence of metallic and insulating states.

IV. SUMMARY

We have studied the Mott transition in the three-orbital Hubbard model. By using the DMFT combined with CT-QMC, we have investigated how the orbital level splitting and the Ising-type Hund's coupling affect the Mott transition in the case of two electrons per site. It has been found that the critical interaction strength shows a nonmonotonic behavior as a function of the level splitting. We have found that this behavior is characteristic for 1/3 filling, in comparison with the previous results at different fillings[15] and for two-orbital models.[24–26] In some parameter regions, the two distinct insulating states, i.e., the MI and the correlated BI, strongly compete with each other, and the metallic state is stabilized there. It can trigger a nontrivial first-order metal-insulator transition, where the insulating state has the intermediate characters between MI and BI. We have also found that the two insulating phases show different behaviors in the phase boundary with the metallic state in the interaction-temperature plane. This difference is reflected in the quasiparticle behavior around the transition. The quasiparticle state around the transition to the MI is suppressed with increasing temperature, while the quasiparticle state near the correlated BI is rather enhanced.

For larger Hund's coupling, we have also investigated the OSMT, where a part of the bands becomes insulating while the others are still metallic. In the transition from the metal to the OSMI phase, the strong renormalization of the orbital level splitting occurs, making its character similar to that of a filling-control Mott transition. On the other hand, the phase transition between the OSMI phase and the MI phase can be simply described by an effective two-band Hubbard model at quarter filling, where the interaction strength of the phase transition is almost independent of Δ, but is substantially reduced by the Hund's coupling between the different orbitals. In the OSMI, the tendency to the non-Fermi liquid has been seen in the self-energy, which is consistent with the previous study at zero temperature.[12]

We have neglected the possibility of magnetic/orbital ordering for simplicity in this paper. It is interesting and important to elucidate how such orderings are incorporated in the metal-insulator transitions discussed here, which is now under consideration.

ACKNOWLEDGMENTS

This research is granted by the Japan Society for the Promotion of Science (JSPS) through the "Funding Program for World-Leading Innovative R&D on Science and Technology (FIRST Program)," initiated by the Council for Science and Technology Policy (CSTP). N.K. is also supported by the Grant-in-Aid for Scientific Research (Grants No. 21540359 and No. 20102008) and the Global Center of Excellence (COE) Program "The Next Generation of Physics, Spun from Universality and Emergence" from the Ministry of Education, Culture, Sports, Science and Technology (MEXT) of Japan. T.O. is supported by the Grant-in-Aid for Scientific Research (Grants No. 21740232 and No. 20104010) and the Next Generation Super Computing Project "Nanoscience Program" from the MEXT of Japan.

*kita@scphys.kyoto-u.ac.jp

[1] Y. Kamihara, T. Watanabe, M. Hirano, and H. Hosono, J. Am. Chem. Soc. **130**, 3296 (2008).
[2] K. Haule and G. Kotliar, New J. Phys. **11**, 025021 (2009)
[3] M. Aichhorn, L. Pourovskii, V. Vildosola, M. Ferrero, O. Parcollet, T. Miyake, A. Georges, and S. Biermann, Phys. Rev. B **80**, 085101 (2009).
[4] P. Richard *et al.*, Phys. Rev. Lett. **102**, 047003 (2009).
[5] A. Hackl and M. Vojta, New J. Phys. **11**, 055064 (2009).
[6] V. Anisimov, I. Nekrasov, D. Kondakov, T. Rice, and M. Sigrist, Eur. Phys. J. B **25**, 191 (2002).
[7] A. Koga, N. Kawakami, T. M. Rice, and M. Sigrist, Phys. Rev. Lett. **92**, 216402 (2004).
[8] A. Koga, K. Inaba, and N. Kawakami, Prog. Theor. Phys. Suppl. **160**, 253 (2005).

[9]C. Knecht, N. Blümer, and P. G. J. van Dongen, Phys. Rev. B **72**, 081103 (2005).
[10]R. Arita and K. Held, Phys. Rev. B **72**, 201102 (2005).
[11]K. Inaba and A. Koga, Phys. Rev. B **73**, 155106 (2006).
[12]L. de' Medici, S. R. Hassan, M. Capone, and X. Dai, Phys. Rev. Lett. **102**, 126401 (2009).
[13]L. de' Medici, Phys. Rev. B **83**, 205112 (2011).
[14]P. Werner, E. Gull, M. Troyer, and A. J. Millis, Phys. Rev. Lett. **101**, 166405 (2008).
[15]P. Werner, E. Gull, and A. J. Millis, Phys. Rev. B **79**, 115119 (2009).
[16]C.-K. Chan, P. Werner, and A. J. Millis, Phys. Rev. B **80**, 235114 (2009).
[17]A. M. Läuchli and P. Werner, Phys. Rev. B **80**, 235117 (2009).
[18]J. P. Lu, Phys. Rev. B **49**, 5687 (1994).
[19]M. J. Rozenberg, Phys. Rev. B **55**, R4855 (1997).
[20]J. E. Han, M. Jarrell, and D. L. Cox, Phys. Rev. B **58**, R4199 (1998).
[21]Y. Ono, M. Potthoff, and R. Bulla, Phys. Rev. B **67**, 035119 (2003).
[22]A. Koga, Y. Imai, and N. Kawakami, Phys. Rev. B **66**, 165107 (2002).
[23]A. Koga, T. Ohashi, Y. Imai, S. Suga, and N. Kawakami, J. Phys. Soc. Jpn. **72**, 1306 (2003).
[24]A. I. Poteryaev, M. Ferrero, A. Georges, and O. Parcollet, Phys. Rev. B **78**, 045115 (2008).
[25]N. Manini, G. E. Santoro, A. Dal Corso, and E. Tosatti, Phys. Rev. B **66**, 115107 (2002).
[26]P. Werner and A. J. Millis, Phys. Rev. Lett. **99**, 126405 (2007).
[27]A. Georges, G. Kotliar, W. Krauth, and M. J. Rozenberg, Rev. Mod. Phys. **68**, 13 (1996).
[28]P. Werner, A. Comanac, L. de' Medici, M. Troyer, and A. J. Millis, Phys. Rev. Lett. **97**, 076405 (2006).
[29]P. Werner and A. J. Millis, Phys. Rev. B **74**, 155107 (2006).
[30]K. Haule, Phys. Rev. B **75**, 155113 (2007).
[31]E. Gull, P. Werner, A. Millis, and M. Troyer, Phys. Rev. B **76**, 235123 (2007).
[32]E. Gull, A. J. Millis, A. I. Lichtenstein, A. N. Rubtsov, M. Troyer, and P. Werner, Rev. Mod. Phys. **83**, 349 (2011).
[33]In the large isotropic Hund's coupling region ($J/U \geqslant 0.25$), the first-order (second-order) transition was suggested in Refs. 11 and 21 (Ref. 46).
[34]We denote the first-order transition point determined from the cusp of the free energy as U_c and that determined with increasing (decreasing) U as U_{c2} (U_{c1}) in this paper. When the crossover occurs in the system, we denote the characteristic interaction strength of the crossover as U_c.
[35]K. Inaba and A. Koga, J. Phys. Soc. Jpn. **76**, 094712 (2007).
[36]J. Bünemann and W. Weber, Phys. Rev. B **55**, 4011 (1997).
[37]J. Bünemann, W. Weber, and F. Gebhard, Phys. Rev. B **57**, 6896 (1998).
[38]F. Lechermann, A. Georges, G. Kotliar, and O. Parcollet, Phys. Rev. B **76**, 155102 (2007).
[39]L. de' Medici, J. Mravlje, and A. Georges, e-print arXiv:1106.0815.
[40]H. Hafermann, K. R. Patton, and P. Werner, e-print arXiv:1108.1936.
[41]L. de' Medici, A. Georges, and S. Biermann, Phys. Rev. B **72**, 205124 (2005).
[42]A. Koga, N. Kawakami, T. Rice, and M. Sigrist, Physica B **359-361**, 1366 (2005).
[43]S. Biermann, L. de' Medici, and A. Georges, Phys. Rev. Lett. **95**, 206401 (2005).
[44]A. Liebsch, Phys. Rev. Lett. **95**, 116402 (2005).
[45]M. Jarrell and J. E. Gubernatis, Phys. Rep. **269**, 133 (1996).
[46]Th. Pruschke and R. Bulla, Eur. Phys. J. B **44**, 217 (2005).